

Improved AlGaIn/GaN HEMTs Grown on Si Substrates Using Stacked AlGaIn/AlN Interlayer by MOCVD

WANG Yong(王勇)^{1,2**}, YU Nai-Sen(于乃森)², LI Ming(黎明)², LAU Kei-May(刘纪美)²

¹National Key Lab on High Power Semiconductor Lasers, Changchun University of Science and Technology, Changchun 130022

²Photonics Technology Center, Department of Electronic and Computer Engineering, Hong Kong University of Science and Technology, Clear Water Bay, Kowloon, Hong Kong

(Received 27 May 2010)

AlGaIn/GaN high electron mobility transistors (HEMTs) are grown on 2-inch Si (111) substrates by MOCVD. The stacked AlGaIn/AlN interlayer with different AlGaIn thickness and indium surfactant doped is designed and optimized to relieve the tensile stress during GaN epitaxial growth. The top 1.0 μm GaN buffer layer grown on the optimized AlGaIn/AlN interlayer shows a crack-free and shining surface. The XRD results show that GaN(002) FWHM is 480 arcsec and GaN(102) FWHM is 900 arcsec. The AlGaIn/GaN HEMTs with optimized and non-optimized AlGaIn/AlN interlayer are grown and processed for comparison and the dc and rf characteristics are characterized. For the dc characteristics of the device with optimized AlGaIn/AlN interlayer, maximum drain current density I_{dss} of 737 mA/mm, peak transconductance G_m of 185 mS/mm, drain leakage current density I_{ds} of 1.7 $\mu\text{A}/\text{mm}$, gate leakage current density I_{gs} of 24.8 $\mu\text{A}/\text{mm}$ and off-state breakdown voltage V_{BR} of 67 V are achieved with $L_g/W_g/L_{gs}/L_{gd} = 1/10/1/1 \mu\text{m}$. For the small signal rf characteristics of the device with optimized AlGaIn/AlN interlayer, current gain cutoff frequency f_T of 8.3 GHz and power gain cutoff frequency f_{max} of 19.9 GHz are achieved with $L_g/W_g/L_{gs}/L_{gd} = 1/100/1/1 \mu\text{m}$. Furthermore, the best rf performance with f_T of 14.5 GHz and f_{max} of 37.3 GHz is achieved with a reduced gate length of 0.7 μm .

PACS: 71.55.Eq, 71.55.Ak, 73.40.Kp

DOI: 10.1088/0256-307X/28/5/057102

With a wide band gap, high breakdown field, high thermal conductivity, large saturated velocity and excellent electron transport performance, AlGaIn/GaN High electron mobility transistors (HEMTs) are very promising in the applications of high-power, high-breakdown voltage,^[1,2] high-frequency, high speed and high efficiency operation,^[3–5] especially in microwave power devices.^[6] As the substrate for GaN growth, sapphire has the bottleneck of bad thermal conduction, which limits the improvement of power density of the AlGaIn/GaN HEMT device and SiC substrates are so expensive that it hinders the application of the GaN material. Therefore, Si is the best alternative substrate for its low cost, good thermal conductivity and integration with the mature Si-based processing techniques.^[7,8]

Because of the large differences of lattice constants and thermal expansion coefficients between the GaN epilayer and the Si substrate, the high dislocation density and bad stress state exist in the GaN epilayer grown on the Si substrate, which results in the bad GaN quality and cracked surface morphology.^[9–11] Compared with those on SiC or sapphire substrates, AlGaIn/GaN HEMTs grown on Si substrates suffer from poorer crystalline quality, smaller critical-layer thickness and higher buffer leakage current density, which limit their applications.

The performance of AlGaIn/GaN HEMT devices is seriously affected by the quality and surface morphology of the GaN buffer layer. In order to improve GaN

quality, relieve the tensile stress, increase the critical thickness of continuous GaN buffer layer and obtain crack-free surface morphology, the structure of bottom layers for HEMT growth should be optimized. It was reported^[12–14] that LT AlN interlayer could be used to relieve the tensile stress in the GaN layer grown on the Si substrate and so as to reduce the cracks in the grown GaN epilayer. In addition, it could also block the spreading of the edge and mixed dislocations from the substrate to the GaN epilayer.

In this work, the stacked AlGaIn/AlN interlayer was designed and optimized to relieve the tensile stress during GaN epitaxial growth. The AlGaIn/GaN HEMTs with optimized and non-optimized AlGaIn/AlN interlayer were grown and processed for comparison and the dc and rf characteristics were characterized.

The AlGaIn/GaN HEMTs were grown on Si (111) substrates by low-pressure MOCVD in an Aixtron 2000HT system. Trimethylgallium (TMGa), trimethylaluminum (TMAI), trimethylindium (TMIn) and ammonia (NH₃) were used as the Ga, Al, In and N precursors, respectively. Biscyclopentadienyl magnesium (Cp₂Mg) and silane (SiH₄) were used as the p- and n-type doping sources. H₂ or N₂ is served as the carrier gas. The 2-inch Si (111) substrates with high resistivity of more than 3000 $\Omega\text{-cm}$ and the thickness of 280 μm were chosen. Before the Si substrates were loaded into the growth chamber of the MOCVD system, they were cleaned by the standard cleaning pro-

**Email: eeywang@gmail.com

cess of Radio Corporation of America (RCA). Prior to growth, the substrates were heated up to 1190°C for 10 min under the H₂ ambience to remove the native oxide on the surfaces of the Si substrates. Then around 40 nm AlN nucleation layer was grown at 1150°C for initiation of GaN growth on the Si(111) substrates, followed by the SiN_x mask layer grown at 1160°C on top of the AlN nucleation layers. Then 0.8 μm undoped GaN transition layer was grown at 1170°C by vertical growth on the exposed AlN nucleation layer and lateral overgrowth on the SiN_x mask layer. After that, the stacked AlGa_N/AlN interlayer was grown on the 0.8 μm GaN transition layer to further reduce the tensile stress, with growth temperature of 950°C for AlN and 1150°C for AlGa_N. Subsequently, continuous 1.0 μm GaN buffer layer was grown at 1170°C on the AlGa_N/AlN interlayer. Finally the HEMT structure was grown on top of the continuous 1.0 μm GaN buffer layer. The typical HEMT structure consists of a 1 nm AlN spacer layer, a 2 nm undoped AlGa_N spacer layer, a 15 nm Si-doped carrier supplying layer and a 3 nm undoped cap layer, with Al composition of 30% and modulation-doped Si concentration of $5 \times 10^{18} \text{ cm}^{-3}$.

In order to more effectively release the tensile stress, the stacked AlGa_N/AlN interlayer was optimized for growth of the top continuous GaN buffer layer. The bottom 10 nm AlN in the stacked layers was grown with growth temperature of 950°C and growth pressure of 100 mbar and the top AlGa_N layer was calibrated with different thickness. The growth temperature and pressure of AlGa_N layer were 1150°C and 100 mbar, same as those of the AlN nucleation layer, in order to decrease the parasitic reaction be-

ing at low temperature and high pressure. The initially optimized results of AlGa_N/AlN interlayer with AlGa_N thickness of 500 nm was reported,^[15] and the optical micrographs, TEM images and Raman spectra of GaN with optimized AlGa_N/AlN interlayer (AlGa_N:500 nm) and with non-optimized AlGa_N/AlN interlayer (AlGa_N:0 nm, namely, only single AlN interlayer) were compared. In this Letter, the stacked AlGa_N/AlN interlayer is further optimized and the growth thickness of the AlGa_N layer is calibrated with 0 nm (only single AlN interlayer), 125 nm, 250 nm and 500 nm. Afterwards, the indium surfactant is doped in the AlGa_N layer to further improve the GaN quality.

AlGa_N/GaN HEMT devices with optimized (sample a: 250 nm AlGa_N, with indium surfactant doped) and non-optimized (sample b: 500 nm AlGa_N, without indium surfactant doped) AlGa_N/AlN interlayer were fabricated for comparison. The source and drain ohmic contacts were prepared by evaporating Ti/Al/Ni/Au (20 nm/150 nm/50 nm/80 nm) multi-layer metals in e-beam evaporator, followed by rapid thermal annealing (RTA) at 850°C for 30 s in N₂ ambient. The gate was defined by contact photolithography and formed by evaporating Ni/Au (50 nm/300 nm) metals for Schottky contacts.

The variation of AlGa_N thickness with 0 nm, 125 nm, 250 nm and 500 nm and the effect of indium surfactant on GaN quality of AlGa_N/GaN HEMT samples were studied by XRD measurement and the sample surface was observed by the optical microscope. The GaN quality and surface morphology of AlGa_N/GaN HEMT samples are shown in Table 1.

Table 1. Comparison of the samples with different thickness of AlGa_N interlayer and with and without indium surfactant doped in AlGa_N interlayer by XRD measurement.

Samples	AlGa _N thickness in stacked interlayer (nm)	FWHM of GaN (002) (arcsec)	FWHM of GaN (102) (arcsec)	Surface morphology
Without indium surfactant doped	0	564	1380	Cracked
	125	534	1134	Crack-free
	250	510	984	Crack-free
	500	552	1248	Crack-free
With indium surfactant doped	250	480	900	Crack-free

Table 2. Comparison of RT Hall results of samples (a) and (b).

Samples	R_s (Ω/sq)	Mobility (cm ² /v·s)	N_s (10 ¹³ cm ⁻²)
(a) AlGa _N 250 nm, with In doped	302	1160	-1.78
(b) AlGa _N 500 nm, without In doped	426	900	-1.65

According to Table 1, the sample without AlGa_N in the stacked AlGa_N/AlN interlayer shows the cracked surface^[15] and the worst GaN quality, while all other samples with AlGa_N layer show crack-free surface observed by the optical microscope, which indicate the stacked AlGa_N/AlN interlayer can more effectively release the tensile stress and improve the GaN quality. Additionally, the sample with AlGa_N thickness of 250 nm has better GaN quality than

the samples with 125 nm and 500 nm. Furthermore, the indium surfactant doped in 250 nm AlGa_N interlayer further improves the GaN quality compared with the samples without indium surfactant. Thus it can be concluded that the stacked AlGa_N/AlN interlayer with indium surfactant doped can more effectively release the tensile stress and improve the GaN quality. Thus the optimized AlGa_N/AlN interlayer was achieved with AlGa_N thickness of 250 nm and indium

surfactant doped.

The mercury-probe capacitance-voltage system was employed to characterize the properties of 2DEG in the AlGaN/GaN HEMTs with optimized (sample a) and non-optimized (sample b) AlGaN/AlN interlayer for comparison. The profiles of capacitance versus voltage ($C-V$) and concentration versus thickness ($n-d$) are shown in Figs. 1 and 2. According to the $C-V$ measurement, basically the same HEMT structure with barrier thickness of 20.0 nm and 2DEG concentration of around $1.0 \times 10^{20} \text{ cm}^{-3}$ is achieved for samples a and b. However, the pinch-off voltages of samples a and b are different (-3.5 V and -3.3 V , respectively). It indicates the performance of AlGaN/GaN HEMT device is different between samples a and b, due to the different quality and surface morphology of the GaN buffer layer, caused by the different structure

of the stacked AlGaN/AlN interlayer.

The 2DEG density and mobility of samples a and b ($7 \text{ mm} \times 7 \text{ mm}$) were characterized at room temperature (RT) by the van der Pauw Hall measurement. Ohmic contact was prepared using e-beam evaporated Ti/Al/Ni/Au, followed by annealing at 850°C for 30 s under N_2 ambient. Table 2 shows the comparison of RT Hall results between samples a and b. According to the Hall results, sample a with optimized AlGaN/AlN interlayer shows higher mobility and higher N_s than sample b with the non-optimized AlGaN/AlN interlayer, which indicates that the optimized AlGaN/AlN interlayer can improve quality and surface morphology of the GaN buffer layer, so as to effectively reduce the impurity scattering and enhance the mobility and N_s of AlGaN/GaN HEMT, very consistent with the $C-V$ results.

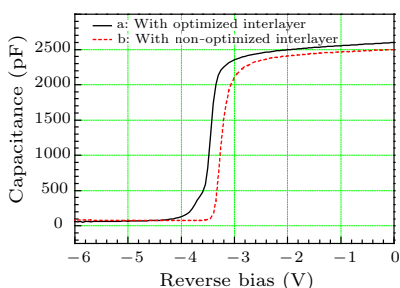


Fig. 1. Mercury-probe $C-V$ profiles of samples (a) and (b).

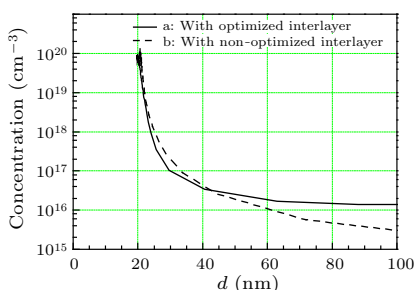


Fig. 2. The 2DEG profiles of samples a and b.

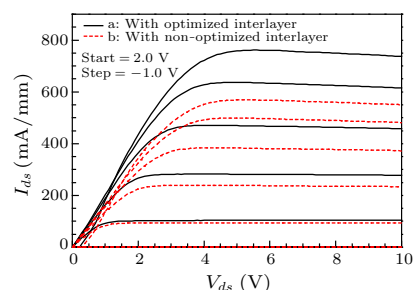


Fig. 3. The dc $I_{ds} - V_{ds}$ characteristics of samples a and b.

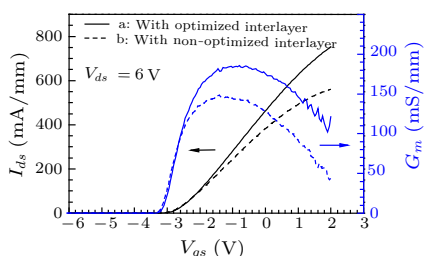


Fig. 4. The dc transfer ($I_{ds} - V_{gs}$) characteristics of samples a and b.

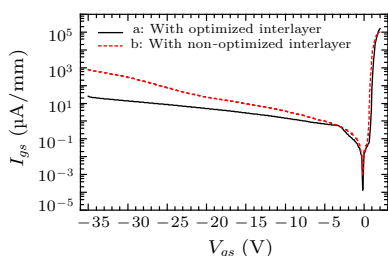


Fig. 5. Gate leakage currents of samples a and b.

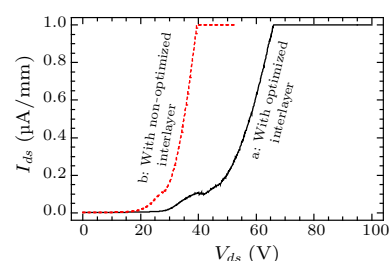


Fig. 6. Off-state breakdown voltages of samples a and b.

Table 3. Comparison of the dc transfer characteristics of samples (a) and (b).

Samples	I_{dss} (mA/mm) @ $V_{gs} = 2.0 \text{ V}$, @ $V_{ds} = 10 \text{ V}$	G_m (mS/mm)	@ V_{gs} (V)	@ V_{ds} (V)	V_{th} (V)	I_{ds} ($\mu\text{A}/\text{mm}$) @ $V_{gs} = -8 \text{ V}$, @ $V_{ds} = 6 \text{ V}$	I_{gs} ($\mu\text{A}/\text{mm}$) @ $V_{gs} = -35 \text{ V}$	V_{BR} (V) @ $I_{ds} = 1 \text{ mA}/\text{mm}$
(a)	737	185	-1	6	-2.6	1.7	24.8	67
(b)	549	148	-2	5	-2.7	2.6	700.8	40

The dc output and transfer characteristics of samples a and b with device dimensions of $L_g/W_g/L_{gs}/L_{gd} = 1/10/1/1 \mu\text{m}$ were measured by using an HP4156A precision semiconductor parameter analyzer. Figures 3–6 show the dc current-voltage ($I_{ds} - V_{ds}$) characteristics, transfer ($I_{ds} - V_{gs}$) characteristics, gate leakage currents and off-state breakdown voltages of samples a and b. The detailed dc

output and transfer characteristics of samples a and b are shown in Table 3 for comparison.

According to Table 3, sample a has a higher maximum drain current density I_{dss} than sample b, which is caused by good surface morphology achieved in sample a with optimized AlGaN/AlN interlayer. Additionally, sample a has lower drain leakage current density I_{ds} and much lower gate leakage cur-

rent density I_{gs} than sample b, which is caused by high resistance in the GaN buffer layer with optimized AlGaIn/AlN interlayer for sample a. Furthermore, sample a achieves a higher off-state breakdown voltage V_{BR} than sample b, resulting from good surface morphology and high resistance in GaN buffer layer grown on optimized AlGaIn/AlN interlayer. The improved dc results of AlGaIn/GaN HEMTs were achieved by using the optimized AlGaIn/AlN interlayer, compared with those reported for the same device dimensions.^[16–19]

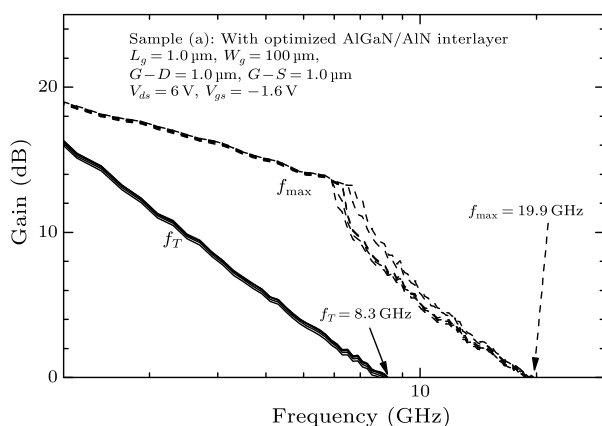


Fig. 7. The rf small signal characteristics of sample (a) with device dimensions of $L_g/W_g/L_{gs}/L_{gd} = 1/100/1/1 \mu\text{m}$.

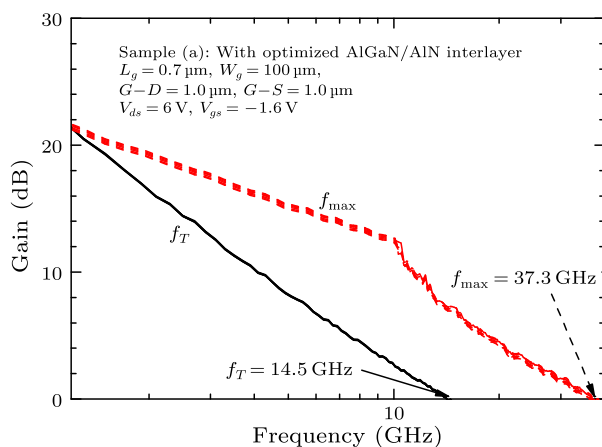


Fig. 8. The rf small signal characteristics of sample a with device dimensions of $L_g/W_g/L_{gs}/L_{gd} = 0.7/100/1/1 \mu\text{m}$.

For high frequency characteristics, on-wafer S -parameter measurements of sample a with the optimized AlGaIn/AlN interlayer were carried out by using an HP 4142B modular dc source/monitor and an Agilent 8722ES network analyzer with Cascade microwave probes. Sample a with device dimensions of $L_g/W_g/L_{gs}/L_{gd} = 1/100/1/1 \mu\text{m}$ and $L_g/W_g/L_{gs}/L_{gd} = 0.7/100/1/1 \mu\text{m}$ were measured. The rf small signal characteristics of the device are plotted in Figs. 7 and 8. The f_T of 8.3 GHz and f_{max} of 19.9 GHz were achieved with dimensions of $L_g/W_g/L_{gs}/L_{gd} = 1/100/1/1 \mu\text{m}$. Further, high rf

performance with f_T of 14.5 GHz and f_{max} of 37.3 GHz was achieved by reducing the gate length to 0.7 μm .

In summary, the stacked AlGaIn/AlN interlayer with AlGaIn thickness of 250 nm and indium surfactant doped can more effectively release the tensile stress and improve the GaN quality. For the dc characteristics, maximum drain current density of 737 mA/mm, peak transconductance of 185 mS/mm, drain leakage current density of 1.7 $\mu\text{A}/\text{mm}$, gate leakage current density of 24.8 $\mu\text{A}/\text{mm}$ and off-state breakdown voltage of 67 V were achieved with $L_g/W_g/L_{gs}/L_{gd} = 1/10/1/1 \mu\text{m}$. For the small signal rf characteristics, f_T of 8.3 GHz and f_{max} of 19.9 GHz were achieved with $L_g/W_g/L_{gs}/L_{gd} = 1/100/1/1 \mu\text{m}$. Furthermore, the best rf performance with f_T of 14.5 GHz and f_{max} of 37.3 GHz was achieved with a reduced gate length of 0.7 μm . The improved dc and rf characteristics of AlGaIn/GaN HEMTs were achieved by using the optimized AlGaIn/AlN interlayer.

References

- [1] Yagi S, Shimizu M, Inada M, Yamamoto Y, Piao G, Okumura H, Yano Y, Akutsu N and Ohashi H 2006 *Solid-State Electron.* **50** 1057
- [2] Ikeda N, Li J, Kato K, Kaya S, Kazama T, Kokawa T, Sato Y, Iwami M, Nomura T, Masuda M and Kato S 2008 *Furukawa Rev.* **34** 17
- [3] Shen L, Coffie R, Buttari D, Heikman S, Chakraborty A, Chini A, Keller S, DenBaars S P and Mishra U K 2004 *IEEE Electron Device Lett.* **25** 7
- [4] Boutros K, Regan M, Rowell P, Gotthold D, Birkhahn R and Brar B 2003 *IEEE Int. Electron Devices Meeting* **1251**
- [5] Joshin K, Kikkawa T, Yayashi H, Maniwa T, Yokokawa S, Yokoyama M, Adachi N and Takikawa M A 2003 *IEEE Int. Electron Devices Meeting* **1261**
- [6] Ambacher O, Foutz B, Smart J, Shealy J R, Weimann N G, Chu K, Murphy M, Sierakowski A J, Schaff W J, Eastman L F, Dimitrov R, Mitchel A and Stutzmann M 2000 *J. Appl. Phys.* **87** 334
- [7] Umeno M, Egawa T and Ishikawa H 2001 *Mater. Sci. Semiconduct. Processing* **4** 459
- [8] Wu K T, Chang P H, Lien S T and Chen N C 2006 *Physica E: Low-dimensional Systems and Nanostructures* **32** 566
- [9] Weng X, Raghavan S, Acord J D, Jain A, Dickey E C and Redwing J M 2007 *J. Cryst. Growth* **300** 217
- [10] Dadgar A, Veit P, Schulze F and Blasing J 2007 *Thin Solid Films* **515** 4356
- [11] Liu Z, Wang X L, Hu G X, Guo L C, Li J P, Li J M and Zeng Y P 2007 *J. Cryst. Growth* **298** 281
- [12] Raghavan S, Weng X J, Dickey E and Redwing J M 2005 *Appl. Phys. Lett.* **87** 142101
- [13] Reiher A, Blasing J, Dadgar A, Diez A and Krost A 2003 *J. Cryst. Growth* **248** 563
- [14] Dadgar A, Blasing J, Diez A, Alam A, Heuken M, Krost A 2000 *Jpn. J. Appl. Phys.* **39** L1183
- [15] Wang H, Liang H, Wang Y, NG K W, Deng D M and Lau K M 2010 *Chin. Phys. Lett.* **27** 038103
- [16] Wang M J and Chen K J 2008 *IEEE Int. Electron Devices Meeting (IEDM)*
- [17] Liu J, Zhou Y G, Zhu J, Cai Y, Lau K M and Chen K J 2007 *IEEE Trans. Electron Devices* **54** 2
- [18] Feng Z H, Cai S J, Chen K J and Lau K M 2005 *IEEE Electron Device Lett.* **26** 870
- [19] Luo W J, Wang X L, Xiao H L, Wang C M, Ran J X, Guo L C, Li J P, Liu H X, Chen Y L, Yang F H and Li J M 2008 *Microelectron. J.* **39** 1108